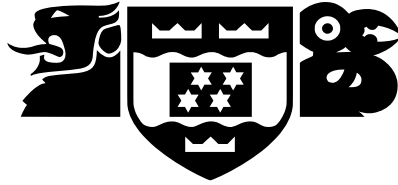


VICTORIA UNIVERSITY OF WELLINGTON  
*Te Whare Wānanga o te Ūpoko o te Ika a Māui*



School of Mathematics and Statistics  
*Te Kura Mātai Tatauranga*

PO Box 600  
Wellington  
New Zealand

Tel: +64 4 463 5341  
Fax: +64 4 463 5045  
Internet: [sms-office@vuw.ac.nz](mailto:sms-office@vuw.ac.nz)

## **Mathematical Modelling of Blood Flow in Arteries**

Elijah Peach

Supervisor: Dimitrios Mitsotakis

Submitted in partial fulfilment of the requirements for  
Masters of Science by Thesis.  
2019

### **Abstract**

Herein contained is an exploration into mathematical modelling pertaining to blood flow in arteries. Previous models are considered as well as a new model derived. Some properties of these new models are investigated. They hold similarities with models from other physically significant systems, namely the KdV/BBM equations used for the modelling of water flow.

# Contents

<b>1</b>	<b>Introduction</b>	<b>1</b>
<b>2</b>	<b>Derivation of current models</b>	<b>4</b>
2.1	Continuity Equation . . . . .	4
2.2	Mass Conservation . . . . .	5
2.3	Momentum Conservation . . . . .	5
2.4	Navier-Stokes Equations . . . . .	7
2.5	1D Models . . . . .	7
2.6	Mass Conservation . . . . .	8
2.7	Momentum Conservation . . . . .	8
2.8	0d Models . . . . .	9
<b>3</b>	<b>Asymptotic Models</b>	<b>13</b>
3.1	Wall Motion . . . . .	15
3.2	Stress-strain relations . . . . .	16
3.3	Asymptotic Analysis . . . . .	17
<b>4</b>	<b>Further Improvements</b>	<b>20</b>
4.1	Improved Boussinesq Systems . . . . .	20
4.2	Addition of a viscosity term . . . . .	21
4.3	Development of the KdV-BBM type equation . . . . .	22
4.4	Solitary Waves . . . . .	24
4.5	Alternative Derivation . . . . .	24
<b>5</b>	<b>Numerical Methods</b>	<b>27</b>
5.1	Spectral Methods . . . . .	27
5.2	Differentiation Matrix . . . . .	27
5.3	Results . . . . .	28
<b>6</b>	<b>Conclusions</b>	<b>31</b>

# List of Figures

1.1	Depiction of the arterial structure. Reproduced from [1]. . . . .	3
2.1	(a) a 3 element Windkessel Model and (b) a 4 element Windkessel Model. Reproduced from [1]. . . . .	11
2.2	Further depictions of the various schematics used for the Windkessel model. More complicated circuits can be constructed from the basic elements and can be used for better modelling, such as (f), similar to a Generalized Maxwell model. Reproduced from [2]. . . . .	12
3.1	Physical domain of the artery . . . . .	14
5.1	Results of the numerical experiments . . . . .	29

# Chapter 1

## Introduction

The study of the human cardiovascular system has been a multidisciplinary approach spanning many years. Though the physical structure was known since antiquity (and many different theories put forward to explain both operation and purpose), the major developments came from William Harvey in 1628. He postulated that the heart was responsible for blood flow in the cardiovascular system. It was this idea that began the modern understanding of the cardiovascular system[3].

The foray of mathematics into this topic concerned itself mainly with modelling the flow of blood in arteries. To this end, Euler began with the formulation of equations to describe these. Still in use today and (appropriately) named the Euler Equations, they describe incompressible and inviscid flow in arteries. Poiseuille's law (given in 1846),  $\frac{\Delta p}{L} = \left(\frac{8\mu}{\pi R^4}\right) Q$  relates pressure drop to flow rate, providing both an accessible and accurate model. Further work by Navier and Stokes led to the development of a set of equations for general motion of a viscous fluid.

Auxiliary to the fluid-flow approach is the lumped parameter model. Developed by Otto Frank,[4] the Windkessel model treats the arteries as an electric circuit, first as a simple resistor, with successive circuit elements like capacitors and inductors added for greater accuracy. Another significant contributor was Womersley, who worked on solutions to the linearized Navier-Stokes equations[5]. More recent developments have been focused around the idea of pulse wave propagation, in which models are derived from waves in the circulatory system having finite speed[1, 6]. Overall, there have been many contributors to this topic, with this being a small recount of a rich history.

Cardiovascular disease stands as a leading cause of death in the world, comparable in toll to other afflictions like cancer. The problems that arise with the vascular system are largely mechanical failures - obstructions due to build-up of plaque, or hardening of the arteries (arteriosclerosis) for example. Understanding when and where these failures occur is vital. Preventive intervention can often minimize or remove some of these problems, and stands as a good strategy to counter heart disease. Thus, anything which helps to understand the mechanics of blood flow can be potentially used as a tool to see out this strategy. Mathematics stands as one of these tools. Mathematical models that simulate blood flow are used in operations and in consideration of devices such as heart stents. In such sensitive cases as surgery, it is important to have a strong theoretical basis on which these operations are performed[7, 8, 9].

Secondary to clinical importance, the cardiovascular system is also rather fascinating. It is an approachable physical system, being abstractly relatable to a system of pipes with a pump attached. From this 'simple' system, the complexity can ramp up quickly, as modelling for the capillaries and veins is added. Further effects such as that of viscosity and viscoelasticity

from the arterial walls can be considered. The study of this topic is self-justifiable, and may have contributed to the rich history of mathematics in haemodynamics. In time I should hope the entire system will be solved; it would make for a great self-contained story.

We are not afforded that luxury yet however.

The cardiovascular system is responsible for maintaining and regulating blood flow. It is comprised of a network of vessels that form a closed loop with the heart. There are two main sections - arteries, which carry blood away from the heart and veins which carry blood to the heart. They link together in the organs of the body through the capillaries - extremely narrow branching beds through which the blood can interface the organs.

Structurally, the two systems are very different - arteries tend to be narrow, high pressure and carry oxygenated blood, while the veins are wider, low pressure and carry deoxygenated blood. The entire system is driven by the heart which acts as a large pump by taking blood into it and contracting to force it out. Figure (1.1) gives a good outline to the structure.

The blood itself is a complex mixture of chemicals. The general role of blood is to act as a transport agent. Any chemical which moves throughout the body will do so through the blood, including both nutrient and waste byproducts. These chemicals are largely transported through the blood plasma, which contains mostly water and accounts for around half of the blood volume. The other half is comprised of blood cells, with majority red. These are large cells which contain hemoglobin, a chemical responsible for the transport of oxygen and carbon dioxide from the organs to the lungs[7].

Blood is a non-newtonian fluid[10] which displays shear-thinning properties. These are related to the microscopic properties and structure of the red blood cells. In this study, we will generally be treating blood as an inviscid fluid, one that does not have viscosity. In the arteries this assumption allows for accurate models, but breaks down in the capillaries, where the size of the vessel and red blood cells are comparable, and the veins, where blood flow is much lower.

The structure of this thesis is first to show and give some models from literature with focus on 1D and 0D. From there, we turn to the formulation of a system derived by asymptotic methods, exploring both their initial formulation and subsequent simplifications. Finally, some properties of the new models are investigated. Results have been published, with work beginning in [11].

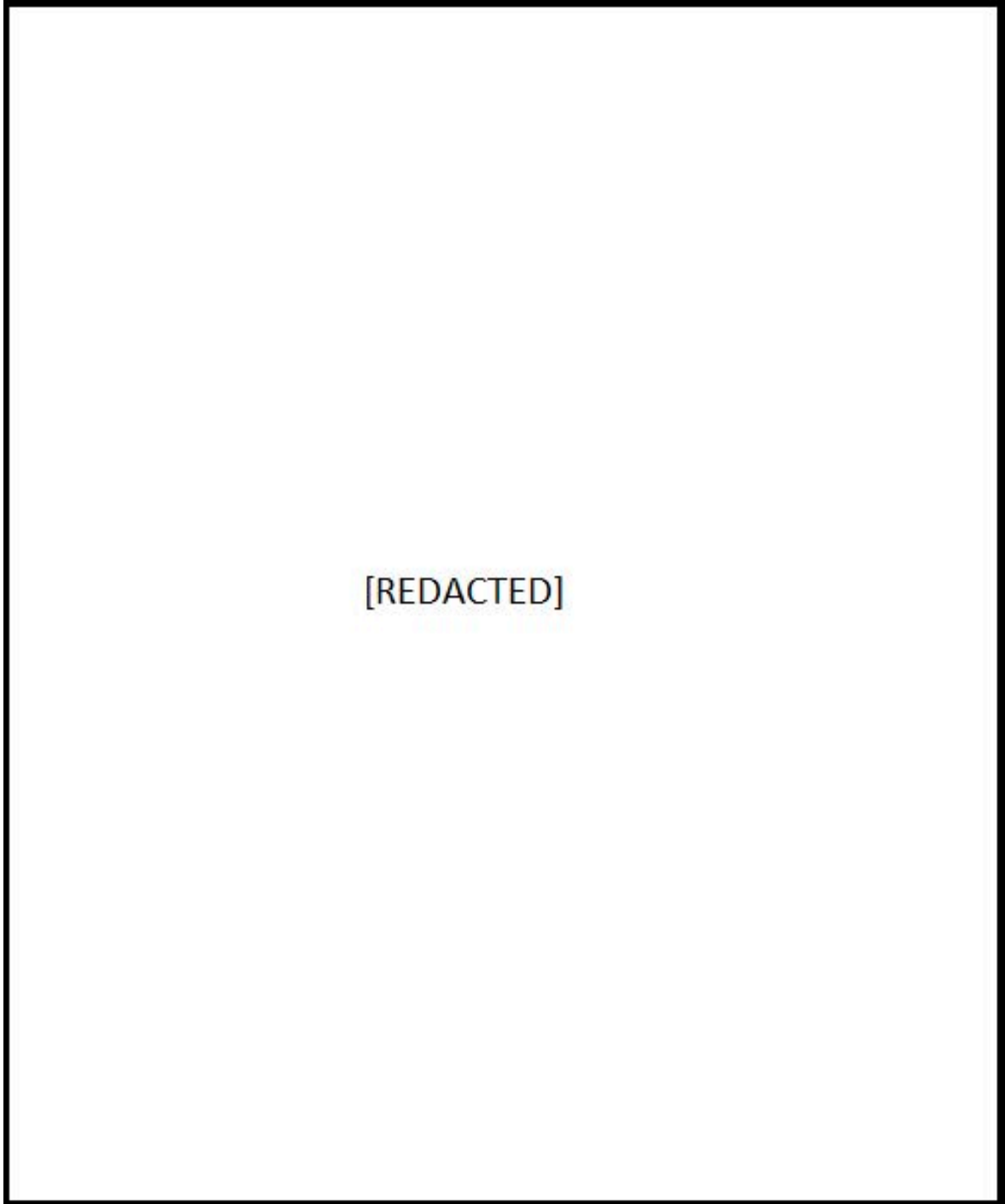


Figure 1.1: Depiction of the arterial structure. Reproduced from [1].

## Chapter 2

# Derivation of current models

Blood flow, like many things, can be described by a set of equations. These equations are the mathematical model we choose. They are derived from the application of empirical laws and logical consequences of them arising from mathematical reasoning and examination. In this chapter I will be showing the derivation of the general laws of motion for fluid flow. These comprise the first major models used[12, 13, 7] and give an example of how mathematical reasoning can be applied to arrive at a model. Some of the methods presented here indeed shall feed into the later chapters, where nondimensionalization is used. Here I shall also discuss the Windkessel model.

### 2.1 Continuity Equation

We begin with a statement: the rate of change of a particular quantity in a given volume is exactly the net migration through the surface, and production/consumption of it inside the system.<sup>1</sup> Mathematically, we write this in terms of integrals as the following:

$$\frac{\partial}{\partial t} \int_V f = - \int_{\partial V} f \mathbf{u} \cdot \mathbf{n} - \int_V s$$

where  $f$  is the quantity,  $\mathbf{u} = [u_{(x)}, u_{(y)}, u_{(z)}]$  is the material velocity vector,  $\mathbf{u} \cdot \mathbf{n}$  is the dot product of the material velocity and unit normal vector to the surface, and  $s$  is the source/sink of the system.

The integrals given are a mathematical formulation involving both the volume and the boundary of the volume. Our goal is to combine the integrals into one statement, as opposed to two separate integrals. To do this, we apply the Divergence Theorem to the surface integral to obtain:

$$\frac{\partial}{\partial t} \int_V f = - \int_V \nabla \cdot (f \mathbf{u}) - \int_V s$$

By assumption, this is over a control volume, so using Reynolds Transport Theorem, the left hand side is transformed to give:

$$\int_V \frac{\partial f}{\partial t} = - \int_V \nabla \cdot (f \mathbf{u}) - \int_V s$$

Essentially, this brings the derivative inside the integral.

Now the integrals are all combined to give:

$$\int_V \left( \frac{\partial f}{\partial t} + \nabla \cdot (f \mathbf{u}) + s \right) = 0$$

---

<sup>1</sup>Heat is a good example of such a quantity

This implies that:

$$\frac{\partial f}{\partial t} + \nabla \cdot (f\mathbf{u}) + s = 0$$

This final equation is the continuity equation, commonly used in the context of quantities that are being preserved such as energy. For the next step, it will be used to derive equations for mass and momentum conservation.

## 2.2 Mass Conservation

Because mass is neither created nor destroyed in any fluids we are concerned with, the rate of change of mass is zero. This is the law of mass conservation. The system will also be treated as closed, so that no mass can enter or leave. We desire a translation of this idea into fluids. The mass of a fluid is given by the integral of the density over a given volume; in this case, the control volume. Considering this and the other statements, we have formally:

$$\frac{\partial}{\partial t} \int_V \rho = 0 \quad (2.1)$$

The quantity in question here is density, which can be substituted into the continuity equation immediately to get:

$$\frac{\partial \rho}{\partial t} + \nabla \cdot (\rho\mathbf{u}) = 0 \quad (2.2)$$

A further simplification can be made here. By treating the fluid as having constant density (as is the case with many liquids like blood) allows a simple statement for the conservation of mass in a fluid;

$$\nabla \cdot \mathbf{u} = 0 \quad (2.3)$$

Note that this condition also gives that the fluid is incompressible.

## 2.3 Momentum Conservation

Momentum can neither be created nor destroyed, only transferred.

A similar calculation for mass will give the momentum of a control volume, using momentum density (also referred to as mass flux) as the conserved quantity as opposed to simply mass density. The initial integral is thus:

$$\frac{\partial}{\partial t} \int_V \rho\mathbf{u} = s$$

Where  $\mathbf{u}$  is the velocity vector of the control volume. This gives us:

$$\frac{\partial(\rho\mathbf{u})}{\partial t} + \nabla \cdot (\rho\mathbf{u} \otimes \mathbf{u}) - s = 0 \quad (2.4)$$

We proceed similarly to the mass conservation - more terms do arise as a result of the product rule from the del operator. By expanding the terms, we arrive at

$$\mathbf{u} \frac{\partial \rho}{\partial t} + \rho \frac{\partial \mathbf{u}}{\partial t} + \mathbf{u} \otimes \mathbf{u} \cdot \nabla \rho + \rho \mathbf{u} \cdot \nabla \mathbf{u} + \rho \mathbf{u} \nabla \cdot \mathbf{u} = s \quad (2.5)$$

Rearranging, we get

$$\mathbf{u} \left( \frac{\partial \rho}{\partial t} + \nabla \cdot (\rho\mathbf{u}) \right) + \rho \left( \frac{\partial \mathbf{u}}{\partial t} + (\mathbf{u} \cdot \nabla) \mathbf{u} \right) = s \quad (2.6)$$



Which, given the mass conservation law, simplifies to

$$\rho\left(\frac{\partial \mathbf{u}}{\partial t} + (\mathbf{u} \cdot \nabla)\mathbf{u}\right) = s \quad (2.7)$$

Unlike in the case with mass conservation, the source term of the momentum conservation is nonzero. This is due to forces acting on the system in some way. These can be categorized into three parts:

**External Force:** Caused by forces acting on the body as a whole. The major (and most commonly accounted for) force is gravity

**Internal Force:** These tend to arise due to interactions of particles with each other. The viscosity of a fluid is an example.

**Surface Stress:** Caused by interactions on the boundary of the fluid. An example of this is blood interacting with the artery. On the boundary, this will be equal to the internal force, and we will capture the influence of the wall via the pressure term.

We account for all these forces in different ways. First, external forces are simply modelled by addition of a term such as  $g$ . In this study, we will consider the body forces as negligible. In the case of a resting body, forces in the arteries are mainly dominated by the heart and arterial compliance, justifying this choice.

It is good to note that this is not the case in many situations. There are a lot of forces that can act on the body which have drastic effects. Microgravity tends to have a detrimental effect on the cardiovascular system, a phenomenon being actively investigated by NASA and which will become more important as mankind ventures further into space[14]. Back on Earth, G-force from jets can lead to redouts, where the pilot simply passes out as the brain is flooded with blood. Even the simple act of running changes the body forces. All these interactions are very complex.

The internal stresses are encoded in a matrix, called the Cauchy stress tensor. All stresses within the material can be described in this matrix; three forces parallel with the coordinates and 6 shear stress components - 3 components in total for each coordinate. These forces will be acting through a surface, so invoking the divergence theorem, we can obtain

$$\int_{\Omega} s = \int_{\partial V} \mathbf{T} \cdot \mathbf{n} + g = \int_V \nabla \cdot \mathbf{T} + \mathbf{f}_{external} \quad (2.8)$$

Now an assumption is made on the nature of  $\mathbf{T}$ . This relation is derived from the mechanical properties of the fluid - it is assumed to be a linear function of the derivative of the velocity. Here, the relation is

$$\mathbf{T} = -PI + \mu(\nabla \mathbf{u} + \nabla \mathbf{u}^T) \quad (2.9)$$

Here  $P$  is the pressure and  $\mu$  the viscosity term. This is known as a constitutive equation. This relation in particular is for Newtonian incompressible fluids, and different equations here will lead to different modelling. It may be a good place to start if one wishes to derive more complex behaviour.

Now we apply the del operator to  $\mathbf{T}$ , and rearrange to obtain:

$$\begin{aligned} \nabla \cdot \mathbf{T} &= -\nabla \cdot PI + \mu \nabla \cdot (\nabla \mathbf{u} + \nabla \mathbf{u}^T) \\ &= -\nabla \cdot PI + \mu \nabla^2 \mathbf{u} + \nabla(\nabla \cdot \mathbf{u}) \\ &= -\nabla \cdot PI + \mu \nabla^2 \mathbf{u} \end{aligned} \quad (2.10)$$

as  $\nabla \cdot \mathbf{u} = 0$  by mass conservation

## 2.4 Navier-Stokes Equations

By combining the two conditions, we finally arrive at:

$$\begin{aligned} \frac{\partial \mathbf{u}}{\partial t} + (\mathbf{u} \cdot \nabla) \mathbf{u} + \nabla \frac{P}{\rho} - \mu \nabla^2 \mathbf{u} &= 0 \\ \nabla \cdot \mathbf{u} &= 0 \end{aligned} \quad (2.11)$$

This set of equations is known as the Navier-Stokes equations, well renowned for their ubiquity in fluid dynamics. Indeed, they are the set of equations which describe all incompressible fluid flow, and are a cornerstone of any study related to it.

Despite having been derived over 100 years ago, the equations are still remain unsolved, owing to their difficulty. The unique phenomenon of turbulence, chaotic movement induced by a number of factors, and high dimensionality are some of these problems. Modelling a full 3D system requires a lot of computer resources and time - resources that may be scarce and time unavailable. In a clinical setting for example, the timescale may be as low as a few hours[15]. Simpler models allow for lower resources and time. An added benefit is that simplified models allow insight to potential non-experts, a major benefit for a cross-disciplinary problem.

Of course then, one doesn't want to get snared and perform a fatal error on the whims of a bad model. There is a fine balancing act between what can and could be solved.

## 2.5 1D Models

Attempts to solve equations such as the Navier-Stokes equations often resort to simplifications. This comes at the price of neglecting some physical behaviour, but can lead to models which capture the principal behaviours of the system in a robust and efficient manner. One such strategy is to lower the dimensionality, solving a 1D/0D model as opposed to 3D. For the arterial system, we will only be dealing with a pipe-like domain - the arteries. To model, it will be convenient to use cylindrical coordinates  $(x, r, \theta)$  rather than  $(x,y,z)$ . For  $(x, r, \theta)$ ,  $x$  is parallel to the direction of blood flow in the artery, while  $r$  is transverse to the direction of blood flow. This allows us to make a number of reductions which simplify the system:

- Axial symmetry eliminates  $\theta$ , with no quantities depending on the angle. This lowers the dimensionality immediately by 1. The tube radius is thus also a function of  $x$  and  $t$ .
- The pressure across each axial section is the same, thus only dependent on  $x$  and  $t$ .
- The  $x$  direction velocity component is dominant with respect to the  $r$  and  $\theta$  velocity component. That is to say, velocity in the direction of  $r$  and  $\theta$  is minimal to the point of negligibility. Further, the velocity can be stated as

$$u_{(x)}(x, r, t) = \bar{u}(x, t) s\left(\frac{r}{R(x)}\right) \quad (2.12)$$

where  $\bar{u}$  is the cross-sectional average velocity and  $s$  is a velocity profile.

- The artery radius can be described by

$$R(x, t) = R_0(x) + \eta(x, t) \quad (2.13)$$

Where  $R(x,t)$  is the radius,  $R_0(x)$  is the reference radius and  $\eta$  is the displacement from the reference radius.

- Body forces are 0.

3 more unknowns are added for simplicity of calculation - A, area, Q, average flux, and P, axial pressure, along with a generic axial section denoted by S. Area and average flux are defined as follows:

$$A = \int_S d\sigma$$

$$Q = \rho \int_S u_{(x)} d\sigma = A\bar{u}$$

From here, the Navier-Stokes equations are integrated along a generic axial section.

## 2.6 Mass Conservation

Using the divergence theorem, we change the integral to

$$\int_{\Omega} \nabla \cdot \mathbf{u} = \int_{\Omega_+} u_x - \int_{\Omega_-} u_x + \int_{\Omega(\text{wall})} \mathbf{u} \cdot \mathbf{n} \quad (2.14)$$

Where  $\Omega$  is the volume of the artery in question. The surfaces of the volume are partitioned into 3 segments -  $\Omega_+$ , the entrance of the vessel,  $\Omega_-$ , the exit of the vessel, and  $\Omega(\text{wall})$  the vessel wall. Along  $\Omega(\text{wall})$ , we assume  $u_x = 0$  - this is known as the no-slip condition. This implies  $\boldsymbol{\eta}_t = \mathbf{u}$ . Using this condition, and the definition of Q, we get

$$\frac{\partial A}{\partial t} + \frac{\partial Q}{\partial x} = 0 \quad (2.15)$$

## 2.7 Momentum Conservation

For the momentum conservation, we have a similar derivation as before, with each term being integrated separately.

Using the Arbitrary Lagrangian Eulerian Transport theorem, we have

$$\int_{\Omega} \frac{\partial u_x}{\partial t} = \frac{d}{dt} \int_{\Omega} u_x - \int_{\partial\Omega} u_x \boldsymbol{\eta}_t \cdot \mathbf{n} = \frac{d}{dt} \int_{\Omega} u_x \quad (2.16)$$

where  $\boldsymbol{\eta}_t$  denotes the boundary speed. Along the axial direction, this is 0, and along the boundary  $u_x = 0$ , hence the boundary integral goes to 0. Using the mean value theorem, we are able to obtain:

$$\frac{d}{dt} \int_{\Omega} u_x = \frac{\partial}{\partial t} [A(x_c) \bar{u}(x_c) dx] + \mathcal{O}(dx) \quad (2.17)$$

By dividing by  $dx$ , taking the limit as  $dx \rightarrow 0$  and using the definition of Q, we finally obtain

$$\lim_{dx \rightarrow 0} \left[ \frac{\partial}{\partial t} [A(x_c) \bar{u}(x_c)] + \mathcal{O}(dx) \right] = \frac{\partial Q}{\partial t} \quad (2.18)$$

Using the divergence theorem, we have

$$\int_{\Omega} \nabla \cdot (u_x \mathbf{u}) = \int_{\partial\Omega} u_x \mathbf{u} \cdot \mathbf{n} = \int_{\Omega_+} u_x^2 - \int_{\Omega_-} u_x^2 + \int_{\Omega(\text{wall})} u_x \boldsymbol{\eta}_t \cdot \mathbf{n} \quad (2.19)$$

As  $u_x$  is 0 along the arterial wall, we rearrange to get

$$\int_{\Omega} \nabla \cdot (u_x \mathbf{u}) = \alpha \frac{\partial}{\partial x} \left( \frac{Q^2}{A} \right) \quad (2.20)$$

where  $\alpha = \frac{\int_S u_x^2 d\sigma}{A \bar{u}^2}$

Usually  $\alpha$  is taken to be 1, or at the very least constant. The pressure is independent of time, which leaves us with

$$\frac{1}{\rho} \int_{\Omega} \frac{\partial P}{\partial x} = \frac{A}{\rho} \frac{\partial P}{\partial x} \quad (2.21)$$

Finally we consider the last term of the momentum equation in the Navier-Stokes (equation 2.11):

$$\int_{\Omega} \nabla^2 u_x = \int_{\partial\Omega} \nabla u_x \cdot \mathbf{n} = \int_{\Omega^+} \frac{\partial u_x}{\partial x} - \int_{\Omega^-} \frac{\partial u_x}{\partial x} + \int_{\Omega(\text{wall})} \nabla u_x \cdot \mathbf{n} \quad (2.22)$$

We assume  $\frac{\partial u_x}{\partial x}$  is small, and split  $\mathbf{n}$  into the x and r components. This gives the approximate equation

$$\int_{\Omega} \nabla^2 u_x \approx \beta \bar{u} = \beta \left( \frac{Q}{A} \right) \quad (2.23)$$

Where  $\beta$  is a friction parameter that depends on the velocity profile chosen.

Put together, these equations are

$$\begin{aligned} \frac{\partial Q}{\partial t} + \alpha \frac{\partial}{\partial x} \left( \frac{Q^2}{A} \right) + \frac{\partial P}{\partial x} + \beta \left( \frac{Q}{A} \right) &= 0 \\ \frac{\partial A}{\partial t} + \frac{\partial Q}{\partial x} &= 0 \end{aligned} \quad (2.24)$$

## 2.8 0d Models

First we adopt a pressure-area relation of the form<sup>2</sup>

$$P = \frac{4\sqrt{\pi}hE}{3A_0(1-\sigma^2)} (\sqrt{A} - \sqrt{A_0}) = \frac{\beta}{A_0} (\sqrt{A} - \sqrt{A_0}) \quad (2.25)$$

Where  $E$  is the Young modulus,  $h$  the wall thickness and  $\sigma$  the Poisson ratio. Substituting this and linearising about the point  $A_0$  we greatly simplify (2.24) to

$$\begin{aligned} C \frac{\partial p}{\partial t} + \frac{\partial q}{\partial x} &= 0 \\ L \frac{\partial q}{\partial t} + \frac{\partial p}{\partial x} &= -Rq \end{aligned} \quad (2.26)$$

where

$$C = \frac{2A\sqrt{A_0}}{\beta}, \quad L = \frac{\rho}{A_0}, \quad R = \frac{\rho\beta}{A_0^2} \quad (2.27)$$

---

<sup>2</sup>note:  $\pi r^2 = A \implies r = \frac{\sqrt{A}}{\sqrt{\pi}}$ . This is a linear relation of strain, stating that the force is simply ratio of change of radius multiplied by a kinematic constant ie the pressure, or strain, is simply  $\frac{\Delta r}{r_0}$  multiplied by the appropriate constants

By integrating over the length of the artery, and assuming the mean pressure and flow are equal to the pressure and flow in, we have the system

$$\begin{aligned} C \frac{dp_{in}}{dt} + q_{out} - q_{in} &= 0 \\ L \frac{dq_{out}}{dt} + Rq_{out} + p_{out} - p_{in} &= 0 \end{aligned} \tag{2.28}$$

This now gives an algebraic expression relating pressure and speed. Given an input pressure and speed, one can calculate an output pressure and speed.

Interestingly, these equations are the same as the ones used for electric circuits, treating  $C$  as capacitance of a capacitor,  $R$  as resistance of a resistor and  $L$  as the inductance of an inductor. The pressure and flow are then voltage and current.

Treating the cardiovascular system as an electrical circuit[16, 5] represents some of the earlier efforts in modelling. It is known as the Windkessel model. It consists of a 2, 3 or 4 element circuit, with combinations of resistors, capacitors and inductors used to construct these circuits. This is used to model a small section of a vessel, then a larger system is constructed by the compound addition of individual elements. This forms a lumped parameter model[17, 18, 19, 20]. In figures (2.1) and (2.2) the various representations for the Windkessel model can be seen.

The correspondence to an electric circuit immediately highlights the inability of this model to account for wave propagation. In this model, all circuit elements will react instantaneously to a change in voltage/current, whereas in the human body the wave takes time to travel through. Wave propagation underpins the mechanics of the arterial system - it is a result of the elastic nature of the system. While these models cannot capture this phenomenon, they still remain useful for coupling to other models.

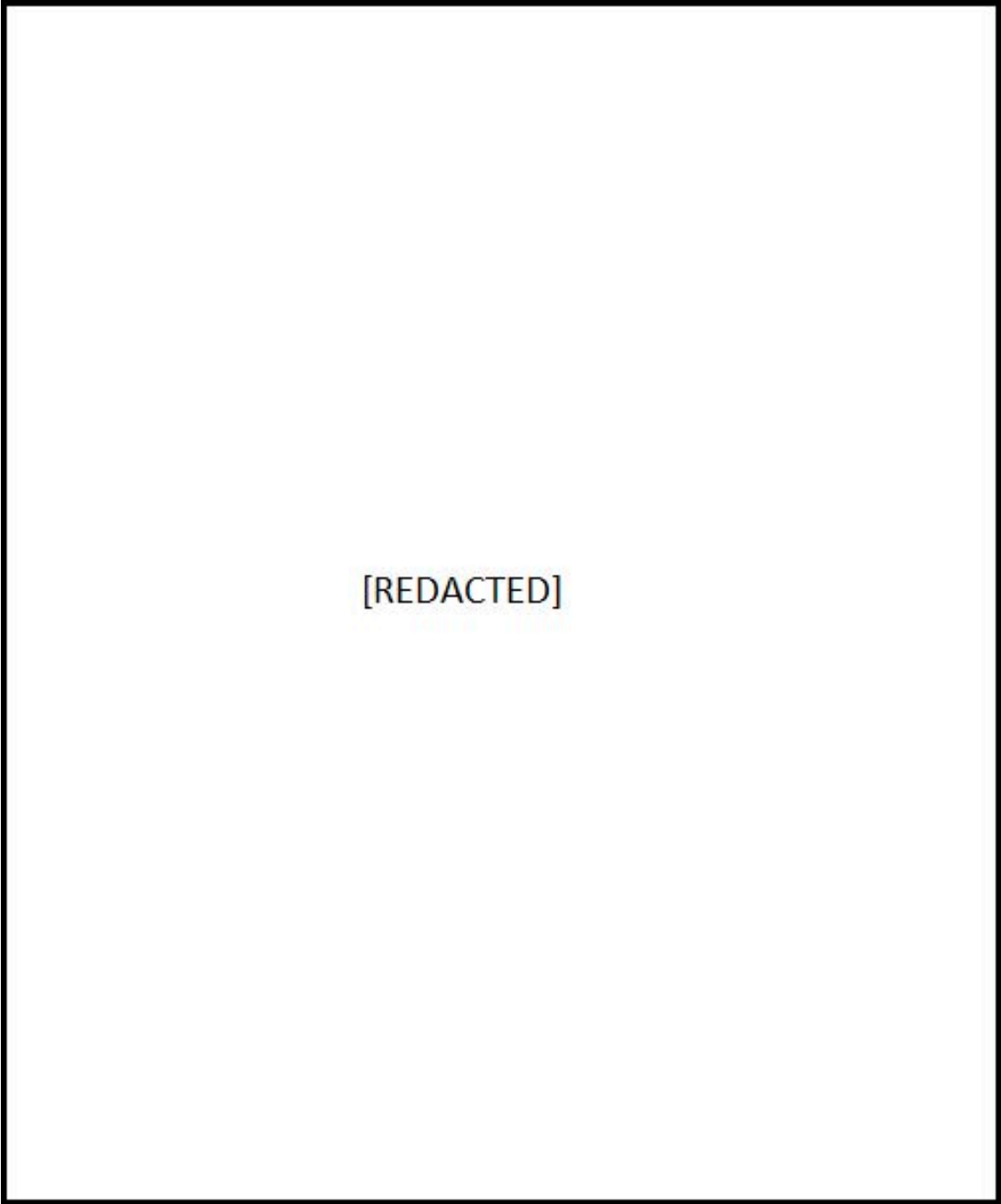


Figure 2.1: (a) a 3 element Windkessel Model and (b) a 4 element Windkessel Model. Reproduced from [1].

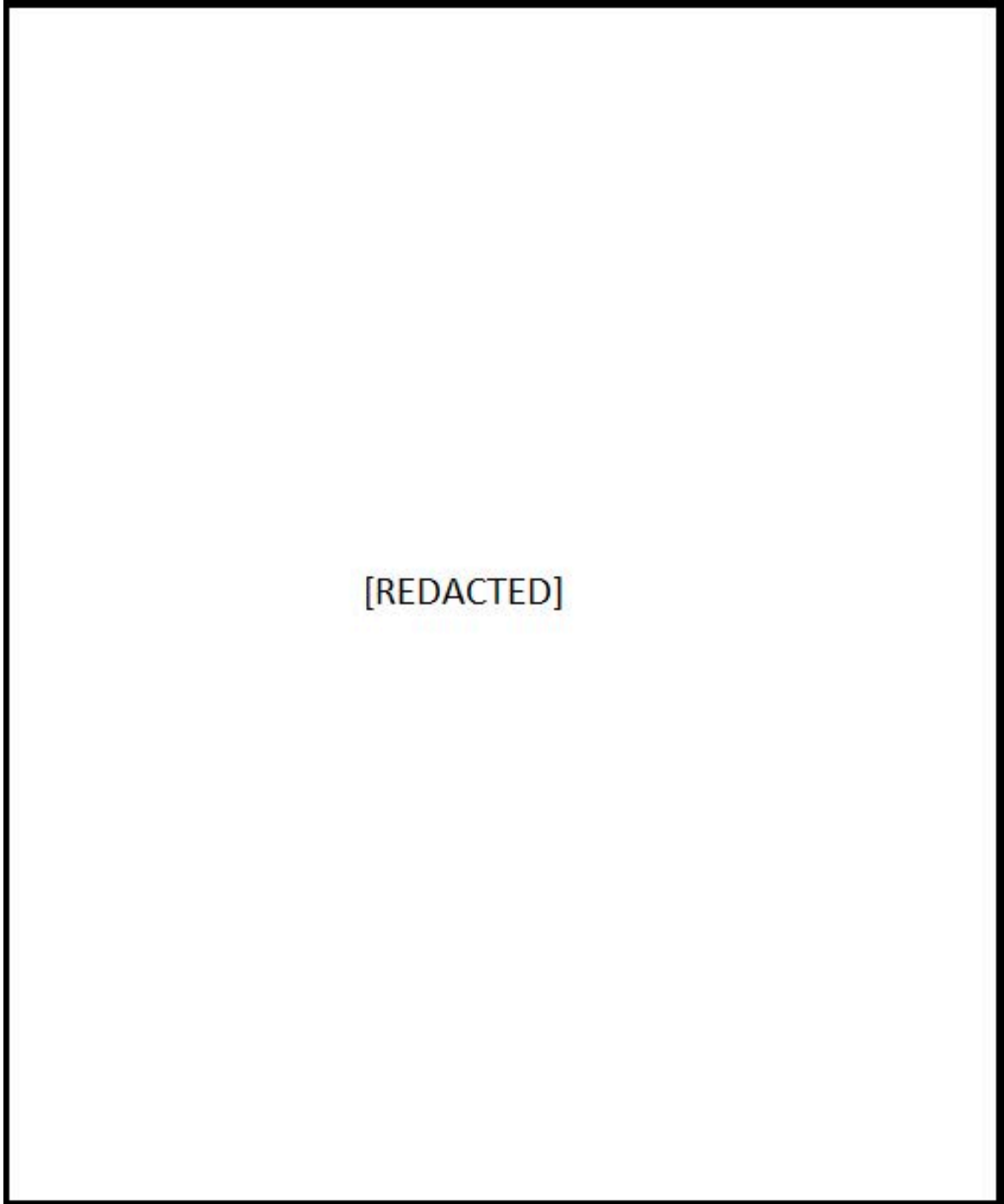


Figure 2.2: Further depictions of the various schematics used for the Windkessel model. More complicated circuits can be constructed from the basic elements and can be used for better modelling, such as (f), similar to a Generalized Maxwell model. Reproduced from [2].

## Chapter 3

# Asymptotic Models

This chapter will focus on the derivation of a newer model that uses asymptotic analysis as the main mathematical method. The methods needed to perform the analysis are presented and then carried out, which give a baseline for the development of a Boussinesq model in the following chapter. We begin with the non-dimensionalization and scaling of the Euler equations. The Euler equations have a similar form to the Navier-Stokes, only they assume the fluid has no viscosity (inviscid flow). In cylindrical coordinates, they are:

$$u_t + uu_x + vv_r + \frac{1}{\rho}p_x = 0 \quad (3.1)$$

$$u_t + uv_x + vv_r + \frac{1}{\rho}p_r = 0 \quad (3.2)$$

$$u_x + v_r + \frac{1}{r}v = 0 \quad (3.3)$$

Where  $u$  is the velocity in the  $x$  direction (parallel to the artery), and  $v$  is the radial velocity (perpendicular to the artery). Flow is assumed to be irrotational, hence velocity with respect to  $\theta$  is 0. Here (and from now on) the subscripts are shorthand for the derivative with respect to that variable ie  $u_t = \frac{\partial u}{\partial t}$ . Scaling and nondimensionalization begins with the series of transformation of variables:

$$\eta^* = \frac{\eta}{a}, \quad x^* = \frac{x}{\lambda}, \quad r^* = \frac{r}{R}, \quad t^* = \frac{t}{T}, \quad (3.4)$$

$$u^* = \frac{u}{\epsilon\tilde{c}}, \quad v^* = \frac{v}{\epsilon\delta\tilde{c}}, \quad p^* = \frac{p}{\epsilon\rho\tilde{c}^2}, \quad \gamma^* = \frac{\gamma}{\rho\lambda\tilde{c}\epsilon}$$

Where:

- $a$  is the amplitude of a typical wave on the wall of the artery
- $\lambda$ , the typical pulse wavelength
- $R$ , the typical vessel radius
- $\tilde{c}$  ( $= \sqrt{Eh/2\rho R}$ ), the Moens-Korteweg characteristic speed
- $T$  ( $= \frac{\lambda}{\tilde{c}}$ ), the time scale chosen
- $\gamma$  is parameter which characterises viscoelasticity <sup>1</sup>

---

<sup>1</sup>The parameter is usually defined in terms of the response a material has when loaded and unloaded with a constant stress. The exact value is both material and model dependent.



- $\epsilon = \frac{a}{R}$
- $\delta = \frac{R}{\lambda}$

The two terms  $\epsilon$  and  $\delta$  characterise the non-linearity and dispersion of the system respectively. The domain these equations pertain to are the arteries, which we can approximate as a long thin tube that does not expand much upon contraction. Taking this into account, inspecting the definition of  $\epsilon$  and  $\delta^2$ , we find these two terms will be very small and of similar order, with the assumptions  $\epsilon \ll 1$  and  $\delta^2 \ll 1$ . Further we assume that  $\epsilon$  and  $\delta^2$  are comparable, with  $\epsilon/\delta^2 = \mathcal{O}(1)$ . This is the Stokes-Ursell number, which characterises the balance between non-linearity and dispersion. By taking  $\mathcal{O}(1)$ , we assume the two effects are balanced. The derivation depends on this, as with a higher Stokes-Ursell number, the model no longer holds as well.

This leads to the cylindrical Euler equations being written as:

$$u_{t^*}^* + \epsilon u^* u_{x^*}^* + \epsilon v^* u_{t^*}^* + p_{u^*}^* = 0 \quad (3.5)$$

$$\delta^2 (v_{t^*}^* + \epsilon u^* v_{t^*}^* + \epsilon v^* v_{r^*}^*) + p_{r^*}^* = 0 \quad (3.6)$$

$$r^* u_{x^*}^* + (r^* v^*)_{r^*} = 0 \quad (3.7)$$

$$\delta^2 v_{x^*}^* = u_{r^*}^* \quad (3.8)$$

With the additional irrotational condition (3.8), and boundary and pressure conditions:

$$v^* = \eta_{t^*}^* + r_{x^*}^{*w} u^* \quad \text{at } r^* = r^{*w} \quad (3.9)$$

$$p^* = \alpha \delta^2 \eta_{t^* t^*}^* + \gamma^* \beta \eta_{t^*}^* + \beta \eta^* \quad \text{at } r^* = r^{*w} \quad (3.10)$$

$$v^* = 0 \quad \text{at } r^* = 0 \quad (3.11)$$

Where  $\alpha = \frac{\rho^w h}{\rho R}$ ,  $\beta = \frac{2R^2}{r_0^2(x)}$ .  $\rho^w$  is the wall density,  $h$  is the wall height, and  $\rho$  is the blood density.  $r^w$  and  $r^{*w}$  are defined as the radius and nondimensionalized radius of the wall respectively. Furthermore, we can define  $r^w(x, t) = r_0(x, t) + \eta(x, t)$ , where  $r_0$  is the reference radius of the artery, and  $\eta$  is the (assumed small) displacement of the wall from  $r_0$ .

From here we begin the analysis. Our aim is to see what order every term is, then try eliminate terms of order  $\mathcal{O}(\epsilon\delta^2, \delta^{>2})$ . To clean up notation, the  $*$  will be dropped.

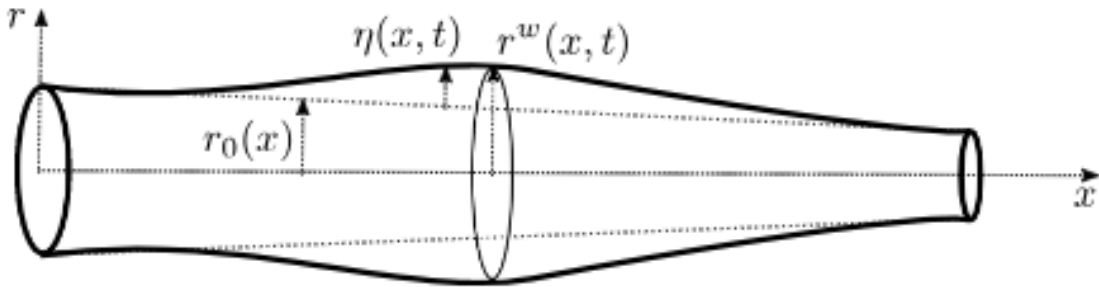


Figure 3.1: Physical domain of the artery

### 3.1 Wall Motion

In this section we will derive equation (3.10). This is the pressure used to describe the wall, and governs its motion. The artery wall has many different layers. We will be approximating it as a thin strip. The study of the fluid-structure interaction is very complex, and gives rise to boundary layer theory, where behaviour changes dramatically depending on how far the fluid is considered to be from the solid surface[21, 22, 23, 24]. To do this, we will consider the forces acting on the wall by considering small elements of it. To this end, we consider the wall thickness ( $\delta r$ , denoted as  $h$ ), arc length ( $r\delta\theta$ ) and wall length ( $\delta x$ ). The volume and mass of the small wall element are then:

$$\delta V = rh\delta\theta\delta x \quad (3.12)$$

$$\delta m = \rho^w \delta V \quad (3.13)$$

Stress,  $\sigma$ , is defined as the force acting on the area of a material. There will be 5 major stresses occurring within the tube, given as pressures. The 5 sources are:

1. Radial Stress,  $\sigma_{(r)}$
2. Axial Stress,  $\sigma_{(x)}$
3. Angular Stress,  $\sigma_{(\theta)}$
4. Fluid Stress,  $p^w$
5. Shear stress,  $\tau^w$

We now consider the forces acting in each direction. The forces must balance in accordance with Newton's laws (mass times acceleration). This will give us equations of motion.

For the radial direction, we have:

$$\delta m \frac{\partial^2 \eta}{\partial t^2} = r\delta\theta\delta x p^w - r\delta\theta\delta x \sigma_{(r)}$$

Simplifying to:

$$\rho^w h \frac{\partial^2 \eta}{\partial t^2} = p^w - \sigma_{(r)} \quad (3.14)$$

The angular acceleration will be 0, as we are assuming cylindrical symmetry. However, as the angular arclengths increase, the radius increases. This is a consequence of cylindrical symmetry - if the arclength between two points increase, it must be that the radius increased. In other words, angular and radial stress are related. To find this relation, we consider the radial and angular stress to be in equilibrium, and set

$$r\delta\theta\sigma_{(r)} = 2hsin\left(\frac{\delta\theta}{2}\right)\sigma_{(\theta)} \quad (3.15)$$

which simplifies to:

$$\sigma_{(r)} = \frac{h}{r}\sigma_{(\theta)} \quad (3.16)$$

We will assume the arteries do not elongate or contract over the cardiac cycle as they are tethered in place, thus the axial acceleration will be 0. Therefore, any stress from this direction will be a constant term, and will not be considered for the moment.

### 3.2 Stress-strain relations

Now we consider the strain in each direction. Strain,  $\omega$ , is a dimensionless quantity defined as the change in length divided by the original length. These equations are similar to those for a linear elastic isotropic material, and express the strain in terms of the stress in each direction. They are (in vector notation):

$$\begin{pmatrix} \omega_{(x)} \\ \omega_{(r)} \\ \omega_{(\theta)} \end{pmatrix} = \frac{1}{E} \begin{pmatrix} \sigma_{(x)} \\ \sigma_{(r)} \\ \sigma_{(\theta)} \end{pmatrix} - \nu \begin{pmatrix} \sigma_{(r)} + \sigma_{(\theta)} \\ \sigma_{(\theta)} + \sigma_{(x)} \\ \sigma_{(x)} + \sigma_{(r)} \end{pmatrix} \quad (3.17)$$

Where  $E$  is Young's modulus and  $\nu$  is Poisson's ratio. We assume the displacements in the artery will remain small. Rearranging to solve for the stress, assuming  $\frac{r}{h} \gg \nu$ , and using the relation for  $\sigma_{(r)}$  and  $\sigma_{(\theta)}$  (namely  $\sigma_{(r)} = \frac{h}{r}\sigma_{(\theta)}$ ), we find

$$\sigma_{(x)} = E\nu(\omega_{(x)} + \nu\omega_{(\theta)}) \quad (3.18)$$

$$\sigma_{(r)} = \frac{hE\nu}{r}(\omega_{(\theta)} + \nu\omega_{(x)}) \quad (3.19)$$

Where  $E\nu = \frac{E}{1-\nu^2}$

Axial strain is caused by change in length of the tube. Under the assumption that the artery remains the same length however, we find the axial strain to be 0. Here I will mention there have been some studies into the longitudinal effects of the arteries[25, 26]. A taut string will behave differently to a loose one. Forces do cause tangential stresses, and the fact that the arteries are already under stress means the pressure term could be affected. Certainly there is a difference in axial stress when comparing the arteries and veins.

For angular strain, strain arises in two ways:

1. Between two points in the artery, the arclength between them increases due to a change in angle. Under the assumption of cylindrical symmetry however, this cannot occur. This would cause the artery to balloon out at one particular wedge. With cylindrical symmetry, each cross-section will always be a circle, preventing this.
2. An arclength increasing in length because of the increase in radius. This arclength increase is not impossible under our assumptions, unlike the previous case, so we must consider it.

For the arclength, the change in length is from  $r\delta\theta$  to  $(r + \eta)\delta\theta$ . Strain is defined as change in length divided by original length. Here we will introduce the viscoelasticity, by adding an extra term into the modelling of the strain, related to the resistivity of the material to change. This is modelled as a strain from both the change in length and the resistance to that change, given as:

$$\omega_{(\theta)} = \frac{1}{r\delta\theta} \left( (r + \eta + \gamma \frac{\partial \eta}{\partial t}) \delta\theta - r\delta\theta \right) \quad (3.20)$$

Where  $\gamma$  is the constant related to the viscoelasticity of the vessel wall.

This simplifies to:

$$\omega_{(\theta)} = \frac{\eta + \gamma\eta_t}{r} \quad (3.21)$$

Substituting in to equations of motion, and taking  $\epsilon_x = 0$  as discussed, we find:

$$\rho^w h \frac{\partial^2 \eta}{\partial t^2} = p^w - \frac{hE\nu}{r^2} (\eta + \gamma\eta_t) \quad (3.22)$$

This gives us an equation for the pressure at the wall purely in terms of the wall motion. Nondimensionalizing this equation, we get (3.10).

### 3.3 Asymptotic Analysis

With the wall derivation fully justified, we are ready to begin analysis. By integrating (3.8) from  $r$  to  $r^w$ , we get

$$u(x, r, t) = u(x, r^w, t) - \delta^2 \int_r^{r^w} v_x(x, \tau, t) d\tau \quad (3.23)$$

Giving us  $u(x, r, t) = u(x, r^w, t) + \mathcal{O}(\delta^2)$ . Equation (3.8) also gives us that  $u_r = \mathcal{O}(\delta^2)$ . By differentiating (3.23) with respect to  $x$  and  $t$ , we get

$$u_x(x, r, t) = u_x(x, r^w, t) + r_x^w u_r(x, r^w, t) + \mathcal{O}(\delta^2) \quad (3.24)$$

$$u_t(x, r, t) = u_t(x, r^w, t) + r_t^w u_r(x, r^w, t) + \mathcal{O}(\delta^2) \quad (3.25)$$

However, since  $u_r = \mathcal{O}(\delta^2)$ , we get

$$u_x(x, r, t) = u_x(x, r^w, t) + \mathcal{O}(\delta^2) \quad (3.26)$$

$$u_t(x, r, t) = u_t(x, r^w, t) + \mathcal{O}(\delta^2) \quad (3.27)$$

Inserting (3.8) into (3.5) gives a simpler form of the momentum equation:

$$u_t + \epsilon u u_x + p_x = \mathcal{O}(\epsilon \delta^2) \quad (3.28)$$

Now we try to derive some approximations for  $v$ . We consider the function

$$\psi(x, r, t) = \frac{1}{r} \int_0^r \tau u(x, \tau, t) d\tau \quad (3.29)$$

To calculate this integral, we use the relation (3.23), giving us

$$\psi(x, r, t) = \frac{r}{2} u(x, r^w, t) + \mathcal{O}(\delta^2) \quad (3.30)$$

This is then used in the integration of (3.7) from 0 to  $r$ , giving

$$v(x, r, t) = \frac{1}{r} \int_0^r \tau u(x, \tau, t) d\tau = -\psi \quad (3.31)$$

$$\implies v(x, r, t) = -\frac{r}{2} u_x(x, r^w, t) + \mathcal{O}(\delta^2) \quad (3.32)$$

Substituting this into (3.9), we get an equation for  $\eta$ :

$$\eta_t = -\left(\frac{1}{2} r^w u_x(x, r^w, t) + r_x^w u(x, r^w, t)\right) + \mathcal{O}(\delta^2) \quad (3.33)$$

From the derivation of the wall pressure laws, a new term is derived, to be added to the original equation. This will affect the derived momentum conservation law. The viscoelasticity constant is assumed to be rather small, and we further assume the order of  $\gamma^*$  can be compared to  $\epsilon$  and  $\delta^2$ , as follows:

$$\mathcal{O}(\gamma^* \delta^2) \approx \mathcal{O}(\gamma^* \epsilon) \approx \mathcal{O}(\epsilon \delta^2) \quad (3.34)$$

From here we wish to calculate the derivatives of the viscoelasticity term; specifically we are looking to calculate  $[\gamma^* \beta(x) \eta_t]_x$ . We start by making the substitution of  $\eta_t$ :

$$\eta_t = -\frac{1}{2} (r^w u_x + 2r_x^w u) + \mathcal{O}(\delta^2) \quad (3.35)$$

Because of the assumption that  $\mathcal{O}(\gamma^*\epsilon)$  is very small, we can make the further assumption that

$$\gamma^*r^w = \gamma^*r_0 + \mathcal{O}(\gamma^*\epsilon, \gamma^*\delta^2) \quad (3.36)$$

Substituting, we get:

$$\gamma^*[\beta(x)\eta_t] = -\gamma^*R^2\left(\frac{r_0}{r_0^2}u_x + 2\frac{r_{0x}}{r_0^2}u\right) \quad (3.37)$$

$$= -\gamma^*R^2\left(\frac{1}{r_0}u_x + 2\frac{r_{0x}}{r_0^2}u\right) \quad (3.38)$$

Now we consider the  $x$  derivative. As  $\gamma^*$  and  $R^2$  are constant with respect to  $x$ , we bring them out and use product/quotient rule to obtain:

$$\left(\frac{u_x}{r_0}\right)_x = \frac{u_{xx}r_0 - r_{0x}u_x}{r_0^2} \quad (3.39)$$

$$\left(\frac{r_{0x}u}{r_0^2}\right)_x = \frac{(r_{xx}u)_x r_0^2 - 2r_{0x}(r_{0x}u)}{r_0^4} \quad (3.40)$$

$$= \frac{(r_{xx}u + r_x u_x)}{r_0^2} - \frac{2}{r_0^2} \cdot \frac{r_{0x}^2 u}{r_0^2} \quad (3.41)$$

giving us

$$\gamma^*[\beta(x)\eta_t]_x = -\frac{\gamma^*\beta(x)}{2} \left[ u_{xx}r_0 + r_{0x}u_x + 2r_{0xx}u - 4\left(\frac{r_{0x}^2 u}{r_0^2}\right) \right] \quad (3.42)$$

(3.32) can be inserted into (3.5) to obtain

$$p_r = \delta^2\left(\frac{r}{2}\right)u_{xt}(x, r^w, t) + \mathcal{O}(\epsilon, \delta^2, \delta^4) \quad (3.43)$$

Integrating this from  $r$  to  $r^w$ , then differentiating with respect to  $x$ , we get

$$p_x(x, r, t) = p_x(x, r^w, t) - \delta^2\left(\frac{(r^w)^2 - (r)^2}{4}\right)u_{xxt}(x, r^w, t) - \delta^2\frac{r^w r_x^w}{2}u_{xt}(x, r^w, t) \quad (3.44)$$

Substituting (3.32) into (3.23) and performing the integration, we get

$$u(x, r, t) = u(x, r^w, t) + \delta^2\frac{(r^w)^2 - (r)^2}{2}u_{xx}(x, r^w, t) + \mathcal{O}(\delta^4) \quad (3.45)$$

Using this, integrating (3.7) again, but from 0 to  $r^w$ , and substituting in (3.33), we get

$$\begin{aligned} r^w(\eta_t + r_x^w u(x, r^w, t)) &= -\frac{1}{2}(r^w)^2 u_x(x, r^w, t) - \frac{\delta^2}{4}(r^w)^3 r_x^w u_{xx}(x, r^w, t) \\ &\quad - \frac{\delta^2}{16}(r^w)^4 u_{xxx}(x, r^w, t) + \mathcal{O}(\delta^4) \end{aligned} \quad (3.46)$$

Which rearranges to:

$$\eta_t + r_x^w u^w + \frac{1}{2}r^w u_x^w + \frac{\delta^2}{4}(r^w)^2 r_x^w u_{xx}^w + \frac{\delta^2}{16}(r^w)^3 u_{xxx}^w = \mathcal{O}(\delta^4) \quad (3.47)$$

This gives the approximate mass conservation.

To get the approximate momentum equation, we substitute in our approximations for pressure, the derivatives of  $u$  and the boundary condition (3.10) to obtain

$$\begin{aligned} u_t^w + [\beta(x)\eta]_x + \epsilon u^w u_x^w - \alpha\delta^2(r_{0x}u_t^w)_x - \frac{\delta^2 r_0 r_{0x}}{2}u_{xt}^w - \\ \frac{\alpha\delta^2}{2}(r_0 u_{xt}^w)_x - \frac{\gamma^*\beta(x)}{2} \left[ u_{xx}^w r_0 + r_{0x}u_x^w + 2r_{0xx}u^w - 4\left(\frac{r_{0x}^2 u^w}{r_0^2}\right) \right] = \mathcal{O}(\epsilon\delta^2, \delta^4) \end{aligned} \quad (3.48)$$

which gives the approximate momentum conservation.

We collect these equations, and substitute in  $r^w = r_0 + \epsilon\eta$  to form the nondimensional system:

$$\eta_t + (r_{0x} + \epsilon\eta_x)u^w + \frac{1}{2}(r_0 + \epsilon\eta)u_x^w + \frac{\delta^2}{4}(r_0)^2(r_{0x})u_{xx}^w + \frac{\delta^2}{16}(r_0)^3u_{xxx}^w = \mathcal{O}(\delta^4) \quad (3.49)$$

$$\begin{aligned} & u_t^w + [\beta(x)\eta]_x + \epsilon u^w u_x^w - \alpha\delta^2(r_{0x}u_t^w)_x - \frac{\delta^2 r_0 r_{0x}}{2} u_{xt}^w - \\ & \frac{\alpha\delta^2}{2}(r_0 u_{xt}^w)_x - \frac{\gamma^* \beta(x)}{2} \left[ u_{xx}^w r_0 + r_{0x} u_x^w + 2r_{0xx} u^w - 4 \left( \frac{r_{0x}^2 u^w}{r_0^2} \right) \right] = \mathcal{O}(\epsilon\delta^2, \delta^4) \end{aligned} \quad (3.50)$$

Or, written in dimensional form and discarding higher order terms:

$$\eta_t + (r_{0x} + \eta_x)u^w + \frac{1}{2}(r_0 + \eta)u_x^w + \frac{1}{4}(r_0)^2(r_{0x})u_{xx}^w + \frac{1}{16}(r_0)^3u_{xxx}^w = 0 \quad (3.51)$$

$$\begin{aligned} & u_t^w + \left[ \frac{Eh}{r_0^2 \rho} \eta \right]_x + u^w u_x^w - \frac{\rho^w h}{\rho} (r_{0x} u_t^w)_x - \frac{r_0 r_{0x}}{2} u_{xt}^w - \\ & \frac{\rho^w h}{\rho} r_0 u_{xt}^w)_x - \frac{\gamma Eh}{2r_0^2 \rho} \left[ u_{xx}^w r_0 + r_{0x} u_x^w + 2r_{0xx} u^w - 4 \left( \frac{r_{0x}^2 u^w}{r_0^2} \right) \right] = 0 \end{aligned} \quad (3.52)$$

This gives us a baseline for a model.

## Chapter 4

# Further Improvements

In this chapter I will use equations (3.51) and (3.52) and attempt to further simplify them. This chapter will centre on this goal and discuss the outcomes of it. Currently, the model contains a highly dispersive term  $u_{xxx}^w$ . Our aim now is to try and reduce this higher order term. This derivation will lead to a new class of systems.

### 4.1 Improved Boussinesq Systems

We reuse the approximation (3.45) and rearrange:

$$u(x, r^w, t) = u(x, r, t) - \delta^2 \frac{(r^w)^2 - (r)^2}{2} u_{xx}(x, r^w, t) + \mathcal{O}(\delta^4) \quad (4.1)$$

By substituting in  $r = \theta r^w$  with  $0 \leq \theta \leq 1$ , and  $u(x, \theta r^w, t) = u^\theta(x, t)$ , we obtain:

$$u^w = u^\theta - \delta^2 \frac{(1 - \theta^2)(r^w)^2}{2} u^\theta + \mathcal{O}(\delta^4) \quad (4.2)$$

This implies that  $u^w = u^\theta + \mathcal{O}(\delta^2)$ . This is substituted into (3.49) and (3.50), and will act mainly to replace  $u^w$  with  $u^\theta$ . This gives us:

$$\eta_t + (r_{0x} + \epsilon \eta_x) u^\theta + \frac{1}{2} (r_0 + \epsilon \eta) u_x^\theta + \frac{\delta^2 (1 - 2\theta^2)}{4} (r_0)^2 (r_{0x}) u_{xx}^w + \frac{\delta^2 (2\theta^2 - 1)}{16} (r_0)^3 u_{xxx}^w = \mathcal{O}(\delta^4, \epsilon \delta^2) \quad (4.3)$$

$$\begin{aligned} & (1 - \delta^2 \alpha r_{0xx}) u_t^\theta + [\beta(x) \eta]_x + \epsilon u^\theta u_x^\theta - \delta^2 r_{0x} (3\alpha + r_0) u_{xt}^\theta - \\ & \frac{(2\alpha + (1 - \theta^2 r_0) r_0)}{4} u_{xxt}^w - \frac{\gamma^* \beta(x)}{2} \left[ u_{xx}^\theta r_0 + r_{0x} u_x^\theta + 2r_{0xx} u^\theta - 4 \left( \frac{r_{0x}^2 u^\theta}{r_0^2} \right) \right] = \mathcal{O}(\epsilon \delta^2, \delta^4) \end{aligned} \quad (4.4)$$

We rearrange the momentum equation (3.33) and reuse equation (3.50) and differentiate them twice with respect to x. By differentiating (3.50), we obtain:

$$r_0 u_{xx}^\theta = -2\eta xxt - 5r_{0xx} u_x^\theta - 4r_{0x} u_{xx}^\theta - 2r_{0xxx} u^\theta + \mathcal{O}(\epsilon, \delta^2) \quad (4.5)$$

and for (3.33), we obtain:

$$u_{xxt}^\theta = -[\beta \eta]_{xxx} + \mathcal{O}(\epsilon \delta^2) \quad (4.6)$$

Now we perform a simple manipulation, by writing

$$\begin{aligned} u_{xxx}^\theta &= \nu u_{xxx}^\theta + (1 - \nu) u_{xxx}^\theta \\ u_{xxt}^\theta &= \mu u_{xxt}^\theta + (1 - \mu) u_{xxt}^\theta \end{aligned}$$

We substitute in all of these, to arrive at:

$$\eta_t + (r_{0x} + \epsilon\eta_x)u^\theta + \frac{1}{2}(r_0 + \epsilon\eta)u_x^\theta + A\delta^2 u_{xx}^w + B\delta^2 u_{xxx}^w - C\delta^2(2\eta xxt + 5r_{0xx}u_x^\theta + 4r_{0x}u_{xx}^\theta + 2r_{0xxx}u^\theta) = \mathcal{O}(\delta^4, \epsilon\delta^2) \quad (4.7)$$

$$(1 - \delta^2\alpha r_{0xx})u_t^\theta + [\beta(x)\eta]_x + \epsilon u^\theta u_x^\theta - \delta^2 Du_{xt}^\theta - \delta^2 E[\beta\eta]_{xxx} - \delta^2 F u_{xxt}^w - \frac{\gamma^*\beta(x)}{2} \left[ u_{xx}^\theta r_0 + r_{0x}u_x^\theta + 2r_{0xx}u^\theta - 4\left(\frac{r_{0x}^2 u^\theta}{r_0^2}\right) \right] = \mathcal{O}(\epsilon\delta^2, \delta^4) \quad (4.8)$$

Where:

$$A = \frac{r_0^2 r_{0x}(1 - 2\theta^2)}{4}, \quad B = \frac{r_0^3(2\theta^2 - 1)\nu}{16}, \quad C = \frac{r_0^2(2\theta^2 - 1)(1 - \nu)}{16}$$

$$D = \frac{r_{0x}(3\alpha + r_0)}{2}, \quad E = \frac{(2\alpha + (1 - \theta^2)r_0)r_0\mu}{4}, \quad F = \frac{(2\alpha + (1 - \theta^2)r_0)r_0(1 - \mu)}{4}$$

From here a number of systems can be derived by using different values for  $\theta$ . We are free to choose whatever value of  $\nu$  and  $\mu$  we desire. To obtain the simplest system, we choose  $\nu = \mu = 0$  and  $\theta = \frac{1}{\sqrt{2}}$ . This cancels out many terms, leaving us with:

$$\eta_t + (r_{0x} + \epsilon\eta_x)u^\theta + \frac{1}{2}(r_0 + \epsilon\eta)u_x^\theta = \mathcal{O}(\delta^4, \epsilon\delta^2) \quad (4.9)$$

$$(1 - \delta^2\alpha r_{0xx})u_t^\theta + [\beta(x)\eta]_x + \epsilon u^\theta u_x^\theta - \delta^2 \frac{(3\alpha + r_0)r_{0x}}{2} u_{xt}^\theta - \delta^2 \frac{(4\alpha + r_0)r_0}{8} u_{xxt}^w - \frac{\gamma^*\beta(x)}{2} \left[ u_{xx}^\theta r_0 + r_{0x}u_x^\theta + 2r_{0xx}u^\theta - 4\left(\frac{r_{0x}^2 u^\theta}{r_0^2}\right) \right] = \mathcal{O}(\epsilon\delta^2, \delta^4) \quad (4.10)$$

Now we look to model blood vessels of constant radius. Because of this, any derivatives of the radius with respect to  $x$  will vanish. This greatly simplifies the viscoelastic term, eliminating all but one variable. This gives:

$$\eta_t + \frac{1}{2}(r_0 u_x) + \frac{1}{2}\epsilon\eta u_x^\theta + \epsilon\eta_x u^\theta = \mathcal{O}(\delta^4, \epsilon\delta^2) \quad (4.11)$$

$$u_t^\theta + \beta\eta_x + \epsilon u^\theta u_x^\theta - \delta^2 \frac{(4\alpha + r_0)r_0}{8} u_{xxt}^\theta - \frac{\gamma^*\beta r_0}{2} u_{xx} = \mathcal{O}(\delta^4, \epsilon\delta^2) \quad (4.12)$$

## 4.2 Addition of a viscosity term

As noted above, the Euler equations are very similar to the Navier-Stokes equations, differing only by the viscosity term. Now we seek to account for it.

We use equations (3.5) and (3.6), and perform the same nondimensionalization, only adding in the viscosity term as such:

$$u_{t^*}^* + \epsilon u^* u_{x^*}^* + \epsilon v^* u_{t^*}^* + p_{u^*}^* = \frac{1}{\delta^2} \frac{1}{Re} \left( \frac{1}{r} (ru_r^*)_r + \delta^2 u_{xx}^* \right) \quad (4.13)$$

$$\delta^2 (v_{t^*}^* + \epsilon u^* v_{t^*}^* + \epsilon v^* v_{r^*}^*) + p_{r^*}^* = \frac{1}{Re} \left( \frac{1}{r} (rv_r^*)_r - \frac{v^*}{r^2} + \delta^2 v_{xx}^* \right) \quad (4.14)$$

$$Re = \frac{\lambda \bar{c}}{\kappa}$$

where  $Re$  is defined as the Reynolds number, a dimensionless quantity used to measure turbulence in flow, and  $\kappa$  is the kinematic viscosity. In blood, the Reynolds number is large.



We make the assumption then that  $\frac{1}{Re} = \mathcal{O}(\epsilon\delta^2)$ . Assuming our strategy is to discard any terms  $\mathcal{O}(\epsilon\delta^2, \delta^4)$ , the only term left to consider is  $\frac{1}{r\delta^2 Re}(ru_r)_r$ . The derivation follows a similar pattern to before, by considering the flow as a sum of the wall velocity and higher order terms. By assuming the flow is laminar, and that the flow is described by a suitable velocity profile. This gives:

$$u(x, r, t) = u(x, r^w, t)\phi(x, r, t) + \mathcal{O}(\delta^2) \quad (4.15)$$

This formulation is commonly used to give a description of the flow across the arteries in other systems. Here we are assuming a parabolic flow profile, by taking

$$\phi(x, r, t) = 2\frac{(r^w)^2 - r_0^2}{r_0^2}$$

This then leaves us with:

$$\frac{1}{\delta^2 Re}\left(\frac{1}{r}(ru_r)_r\right) = \frac{-8u^w}{r_0^2\delta^2 Re}$$

As the term is separate and high order, we perform the same reductions as in the previous sections, substituting  $u^w$  for  $u^\theta$ . As it is high order, it has no effect on the high-order assumptions taken such as in equations (3.33) and (3.50).

Adding in this term to equations (4.11) and (4.12), discarding higher order terms and dimensionalizing it, we get:

$$\eta_t + \frac{1}{2}r_0u_x + \frac{1}{2}\eta u_x + \eta_x u = 0 \quad (4.16)$$

$$u_t + \frac{Eh}{\rho r_0^2}\eta_x + uu_x - \frac{(4\rho^w h + \rho r_0)}{8\rho}r_0u_{xxt} + \kappa u - \frac{\gamma Eh}{2\rho r_0}u_{xx} = 0 \quad (4.17)$$

### 4.3 Development of the KdV-BBM type equation

The system (4.16) and (4.17) are re-nondimensionalized using a new set of variables, namely:

$$\eta^* = \frac{\eta}{a}, \quad x^* = \frac{x}{\lambda}, \quad t^* = \frac{t}{T}, \quad u^* = \frac{u}{c_0}$$

where  $T = \frac{2a\lambda}{r_0 c_0}$ ,  $c_0 = \frac{a}{r_0} \sqrt{\frac{2Eh}{\rho R}}$ ,  $\epsilon = \frac{a}{R}$ ,  $\delta = \frac{R}{\lambda}$

The system that arises from these variables is:

$$\eta_{t^*}^* + u_{x^*}^* + 2\epsilon\eta_{x^*}^* = \mathcal{O}(\epsilon^2, \delta^4) \quad (4.18)$$

$$u_{t^*}^* + \eta_{x^*}^* + 2\epsilon u_{x^*}^* u_{x^*}^* - \delta^2 \frac{4\bar{a} + 1}{8} u_{x^* x^* t^*}^* + \epsilon \kappa^* \sigma u^* - \frac{\delta^2 \gamma^*}{\sigma} u_{x^* x^*}^* = \mathcal{O}(\epsilon^2, \delta^4) \quad (4.19)$$

$$\text{Where } \bar{a} = \frac{\rho^w h}{\rho r_0}, \quad \sigma = \frac{2\lambda}{\bar{c}}, \quad \bar{c} = \sqrt{\frac{Eh}{2\rho r_0}}, \quad \kappa^* = \frac{\kappa}{\epsilon}, \quad \gamma^* = \frac{\gamma}{\delta^2}$$

As before, we will drop the asterisks for clarity. By rearranging these equations, we can see that:

$$\eta_t + u_x = \mathcal{O}(\epsilon^2, \delta^4)$$

$$\eta_x + u_t = \mathcal{O}(\epsilon^2, \delta^4)$$

The wave equation  $\eta_{tt} + \eta_{xx} = \mathcal{O}(\epsilon^2, \delta^4)$  follows from this. There are two solutions, but we will be focusing on only one - the wave which propagates to the right ie solutions such that  $\eta_t + \eta_x = \mathcal{O}(\epsilon^2, \delta^4)$ . We can start with the low order approximation  $\eta = u$ . To improve the accuracy, we take higher order terms and assume that:

$$u = \eta + \epsilon A + \delta^2 B + \mathcal{O}(\epsilon^2, \delta^4) \quad (4.20)$$

We substitute this into (4.18) and (4.19) and collect terms of higher order. This leaves us with:

$$\eta_t + \eta_x + \epsilon(A_x + 3\eta\eta_x) + \delta^2(B_x) = \mathcal{O}(\epsilon^2, \delta^4) \quad (4.21)$$

$$\eta_t + \eta_x + \epsilon(A_t + 2\eta\eta_x + \kappa^*\sigma\eta) + \delta^2(B_t - \frac{(4\tilde{\alpha} + 1)}{8}\eta_{xxt} - \frac{\gamma^*}{\sigma}\eta_{xx}) = \mathcal{O}(\epsilon^2, \delta^4) \quad (4.22)$$

In order for these set of equations to hold, the terms of equal order in each separate equation must be equal. Thus we derive:

$$\begin{aligned} A_x + 3\eta\eta_x &= A_t + 2\eta\eta_x + \kappa^*\sigma\eta \\ B_x &= B_t + \frac{(4\tilde{\alpha} + 1)}{8}\eta_{xxt} - \frac{\gamma^*}{\sigma}\eta_{xx} \end{aligned}$$

From here there are a couple of steps. First, we seek to solve for  $A$  and  $B$  by integration. Here we are some freedom to choose integration with respect to  $t$  or  $x$ , depending on which is easier. We make the assumption that  $A_t = -A_x + \mathcal{O}(\epsilon)$  and  $B_t = -B_x + \mathcal{O}(\epsilon)$ . This leads to:

$$\begin{aligned} A &= \frac{-1}{4}\eta^2 + \kappa^*\sigma \int \eta \\ B &= \frac{(4\tilde{\alpha} + 1)}{16}\eta_{xt} - \frac{\gamma^*}{2\sigma}\eta_x \end{aligned}$$

Now we resubstitute these values for  $A$  and  $B$  into equations (4.21) and (4.22) to obtain the KdV-BBM type systems

$$\eta_t + \eta_x + \epsilon\frac{5}{2}\eta\eta_x + \epsilon\frac{\kappa^*\sigma}{2}\eta + \delta^2\frac{4\tilde{\alpha} + 1}{16}\eta_{xxx} - \delta^2\frac{\gamma^*}{2\sigma}\eta_{xx} = \mathcal{O}(\epsilon^2, \delta^4) \quad (4.23)$$

$$\eta_t + \eta_x + \epsilon\frac{5}{2}\eta\eta_x + \epsilon\frac{\kappa^*\sigma}{2}\eta - \delta^2\frac{4\tilde{\alpha} + 1}{16}\eta_{xxt} - \delta^2\frac{\gamma^*}{2\sigma}\eta_{xx} = \mathcal{O}(\epsilon^2, \delta^4) \quad (4.24)$$

Or in dimensional variables

$$\eta_t + \tilde{c}\eta_x + \frac{5\tilde{c}}{2r_0}\eta\eta_x + \kappa\eta + \frac{(4\alpha + 1)\tilde{c}r_0}{16}\eta_{xxx} - \frac{\gamma\tilde{c}^2}{4}\eta_{xx} = 0 \quad (4.25)$$

$$\eta_t + \tilde{c}\eta_x + \frac{5\tilde{c}}{2r_0}\eta\eta_x + \kappa\eta - \frac{(4\alpha + 1)\tilde{c}r_0}{16}\eta_{xxt} - \frac{\gamma\tilde{c}^2}{4}\eta_{xx} = 0 \quad (4.26)$$

The KdV-BBM equations in and of themselves comprise a huge topic. They are used in the modelling of shallow water waves. The BBM equation was derived as an alternative to the KdV equation, and while they are similar, there are some key differences, namely in the solutions and the number of conservative laws. Here I will give a brief recount of a particular solution to the KdV-BBM equation, namely the soliton solution[27].

## 4.4 Solitary Waves

A soliton is a wave which propagates without change in speed or height as they move ie they are a travelling wave solution. They occur when nonlinearity and dispersion cancel out. First, we begin with the general KdV-BBM equation:

$$\eta_t + a_1\eta_x + a_2\eta\eta_x - a_3\eta_{xxt} + a_4\eta_{xxx} = 0 \quad (4.27)$$

As it is a travelling wave, we expect it to have a form reflecting this - as the wave propagates, it remains unchanged:

$$\eta(x, t) = \phi(x - ct) \quad (4.28)$$

We substitute this into the general KdV-BBM equation and make a change of variables  $s = x - ct$ . Using the chain rule, we differentiate with respect to  $s$  to give us the equation

$$-c\phi_s + a_1\phi_s + a_2\phi\phi_s + (ca_3 + a_4)\phi_{sss} = 0 \quad (4.29)$$

Now we integrate, and multiply back through with  $\phi_s$ . This leads to

$$-c\phi\phi_s + a_1\phi\phi_s + \frac{a_2}{2}\phi^2\phi_s + (ca_3 + a_4)\phi_{ss}\phi_s = A\phi_s \quad (4.30)$$

Now one more round of integration will go through without a problem to give:

$$-\frac{c}{2}\phi^2 + \frac{a_1}{2}\phi^2 + \frac{a_2}{6}\phi^3 + \frac{ca_3 + a_4}{2}(\phi_s)^2 = A\phi + B \quad (4.31)$$

Rearranging, this will give the derivative of  $\phi$  as a polynomial of  $\phi$ . This polynomial can change depending on the values for  $A$  and  $B$ , hence many different solutions exist. The wave we desire should be symmetric and decay to 0 as  $s \rightarrow \infty$ . This gives us  $A = B = 0$ , and now we obtain the equation

$$\phi_s^2 = \frac{a_2\phi^2}{3(ca_3 + a_4)} \left( \frac{3(c - a_1)}{a_2} - \phi \right) \quad (4.32)$$

We can solve for  $\phi$  in this ODE by taking the substitution  $g^2 = \frac{3(c-a_1)}{a_2} - \phi$  and using partial fractions. Doing this, we arrive at

$$\phi(s) = \frac{3(c - a_1)}{a_2} \operatorname{sech}^2 \left( \sqrt{\frac{c - a_1}{4(ca_3 + a_4)}} s \right) \quad (4.33)$$

giving the final solution

$$\eta(x, t) = \frac{3(c - a_1)}{a_2} \operatorname{sech}^2 \left( \sqrt{\frac{c - a_1}{4(ca_3 + a_4)}} (x - ct) \right) \quad (4.34)$$

## 4.5 Alternative Derivation

Here we will show an alternative derivation to the KdV-BBM type equations. This will further help to justify the asymptotic model derived. It again relies on the assumption that the flow is irrotational - this is crucial so as for the flow to be described with a smooth velocity potential  $\phi$ . Furthermore, we will choose this profile such that  $u = \phi_x$  and  $v = \phi_y$ .

These are substituted into the cylindrical Euler equations to rewrite them in terms of  $\phi$  as opposed to  $u$  and  $v$ . This gives:

$$\phi_t + \frac{1}{2}\phi_x^2 + \frac{1}{2}\phi_r^2 + \frac{1}{\rho}p + \kappa\phi = 0 \quad (4.35)$$

$$r\phi_{xx} + (r\phi_r)_r = 0 \quad (4.36)$$

The momentum equations are combined to give a single equation, with the second being the mass conservation. The new boundary conditions are:

$$\phi_r = \eta_t + (r_0(x) + \eta)_x \phi_x, \quad \text{for } r = r^w(x, t) \quad (4.37)$$

$$\phi_r = 0, \quad \text{for } r = 0 \quad (4.38)$$

Using the same nondimensionalization variables as (3.4) with the addition that  $\phi^* = \frac{1}{\lambda\epsilon\bar{c}}$ , and performing the same process, we form the nondimensional system:

$$\phi_{t^*}^* + \frac{\epsilon}{2}\phi_{x^*}^{*2} + \frac{\epsilon}{2\delta^2}\phi_{r^*}^{*2} + p^* + \epsilon\kappa^*\phi^* = 0, \quad \text{for } r^* = r^{*w} \quad (4.39)$$

$$r^*\phi_{x^*x^*}^* + (r^*\phi_{r^*}^*)_{r^*} = 0, \quad 0 \leq r^* \leq r^{*w} \quad (4.40)$$

$$\phi_{r^*}^* = 0, \quad \text{for } r^* = 0 \quad (4.41)$$

$$\phi_{r^*}^* = \eta_{t^*}^* + (r_0^*(x^*) + \eta^*)_{x^*} \phi_{x^*}^* \quad \text{for } r^* = r^{*w} \quad (4.42)$$

$$p^* = \delta^2\alpha^*\eta_{t^*t^*}^* + \beta^*(\eta^* + \delta^2\gamma^*\eta_{t^*}^*) \quad \text{for } r^* = r^{*w} \quad (4.43)$$

We will drop the asterisk as before.

Rather than performing a series of integrals to attempt to reduce to discardable higher order terms, this derivation will instead use a series expansion of the velocity potential, as follows:

$$\phi(x, r, t) = \sum_{i=0}^{\infty} r^i \phi_i(x, t) \quad (4.44)$$

By substituting this into equation (4.40), we obtain a recurrence relation, namely:

$$\begin{aligned} \delta^2(\phi_{2i})_{xx} + (2i+2)^2\phi_{2i+2} &= 0 \\ \phi_{2i+1} &= 0 \end{aligned} \quad (4.45)$$

The recurrence relation allows us to build up functions from  $\phi_0$ , allowing us to rewrite  $\phi_i$  purely in terms of  $\phi_0$  and subsequent derivatives. In particular, we arrive at the two following equations:

$$\phi_2 = -\frac{\delta^2}{4}(\phi_0)_{xx} \quad (= \mathcal{O}(\delta^2)) \quad (4.46)$$

$$\phi_4 = \frac{\delta^4}{(6)^2(4)^2}(\phi_2)_{xxxx} \quad (= \mathcal{O}(\delta^4)) \quad (4.47)$$

Any terms for  $i \geq 2$  are guaranteed to be  $\mathcal{O}(\delta^4)$  or higher, hence we may discard them. This leads to the approximation:

$$\phi(x, r, t) = (\phi_0)(x, t) - \delta^2 \frac{r^2}{4} \phi_{0xx}(x, t) + \mathcal{O}(\delta^4) \quad (4.48)$$

The form of equation (4.48) is very similar to (3.45), and the methods used are mimicked here - by this I mean substituting in low-order approximations and then discarding higher

terms when they arise, such as  $\delta^4$ . We substitute (4.48) into (4.43), then (4.43) into (4.39) and eliminate pressure to obtain:

$$\eta_t + r_x^w \phi_{0x} + \frac{r^w}{2} \phi_{0xx} - \delta^2 \frac{r_0^2 r_{0x}}{4} \phi_{0xxx} - \delta^2 \frac{r_0^3}{16} \phi_{0xxxx} = \mathcal{O}(\delta^4, \epsilon \delta^2) \quad (4.49)$$

$$\phi_{0t} - \delta^2 \frac{r_0^2}{4} \phi_{0xxt} + \frac{\epsilon}{2} \phi_{0x}^2 + \epsilon \kappa \phi_0 + \alpha \delta^2 \eta_{tt} + \beta (\eta + \delta^2 \gamma \eta_t) = \mathcal{O}(\delta^4, \epsilon \delta^2) \quad (4.50)$$

These two equations have the same form as the equations (3.51) and (3.52), and help to verify the models.

# Chapter 5

## Numerical Methods

In this section first I will give some background on the methods used to solve the equations derived in previous chapters, and show some results of this. The numerical methods help to solve otherwise intractable equations and validate models.

### 5.1 Spectral Methods

Many different methods exist to solve equations in a general sense. For this, we will focus on a specific strategy known as a spectral method. The method is well suited for solving equation (4.26) due to its form.

### 5.2 Differentiation Matrix

Suppose a curve is described by two vectors -  $[x_1, \dots, x_n]$  and  $[y_1, \dots, y_n]$  - containing the  $x$  coordinates and corresponding  $y$  coordinates respectively. What then is the derivative of this curve at each point? From the Taylor expansion, we know the derivative can be approximated by a finite difference method, specifically:

$$y'_i = \frac{y_{i+1} - y_{i-1}}{2h} \tag{5.1}$$

where  $h = x_i - x_{i-1} = \Delta x$  is constant. Assuming then the solution is periodic, we can rewrite this relation as a matrix:

$$\begin{bmatrix} y'_1 \\ \vdots \\ y'_n \end{bmatrix} = \frac{1}{h} \begin{bmatrix} 0 & \frac{1}{2} & & & -\frac{1}{2} \\ -\frac{1}{2} & 0 & \ddots & & \\ & & \ddots & & \\ & & & 0 & \frac{1}{2} \\ \frac{1}{2} & & & -\frac{1}{2} & 0 \end{bmatrix} \begin{bmatrix} y_1 \\ \vdots \\ y_n \end{bmatrix}$$

This is a second-order finite difference method with error  $\mathcal{O}(h^2)$ . We can represent higher order finite difference schemes as matrices also. There are two points here:

- The derivative can be represented as a polynomial of the function values
- A matrix can be used to represent this derivative

This provides the basis and inspiration for spectral methods - the idea being that this differentiation matrix is taken to the limit to construct an infinite dimensional matrix[28]. All the matrices derived by this are circulant, which in particular describes a convolution. This allows the matrix to be calculated using the Fast Fourier Transform[29].<sup>1</sup>  
We now take equation (4.26) and take the Fourier transform of it:

$$\hat{\eta}_t + ik\tilde{c}\hat{\eta} + \frac{ik}{2} \frac{5\tilde{c}}{2r_0} \hat{\eta}^2 + \kappa\hat{\eta} + k^2 \frac{(4\alpha + 1)\tilde{c}r_0}{16} \hat{\eta}_t + k^2 \frac{\gamma\tilde{c}^2}{4} \hat{\eta} = 0 \quad (5.2)$$

Where  $\hat{\eta}$  is the Fourier transform of  $\eta$ ,  $k$  is the vector of wavenumbers, and from taking the derivative of the Fourier transform, we note:

$$(\hat{\eta}_t) = (\hat{\eta})_t, \quad (\hat{\eta}_x) = ik(\hat{\eta}) \quad (5.3)$$

We can rearrange this equation, and make the substitution  $\hat{\eta}_t = y'$  to give:

$$y' = -16 \frac{(ik\tilde{c}y + \frac{ik}{2} \frac{y\tilde{c}}{2r_0} \text{FFT}(\text{IFFT}(y^2)) + \kappa y + k^2 \frac{\gamma\tilde{c}^2}{4} y)}{(k^2(4\tilde{\alpha} + 1)\tilde{c}r_0)} \quad (5.4)$$

where FFT/IFFT are the Fast Fourier and Inverse Fast Fourier Transform, and division by  $k$  is component-wise.

This equation can be solved as an ODE by an appropriate method such as Runge-Kutta<sup>2</sup>. Once the solution is found in terms of  $y'$ , the IFFT can recover the true solution. This scheme is simple to implement with a fast rate of convergence[28]. In general, this provides a powerful method for solving many different 1D equations by reducing them to ODEs.

### 5.3 Results

In the case that the viscoelasticity and viscosity terms are neglected, the equation contains soliton solutions as derived above. A natural consideration is the effect these two terms have on the propagation of these waveforms.

To do this, we consider an artery with the following parameters:

Radius	r	0.01m
Wall thickness	h	0.0003m
Young Modulus	E	$4.1 \cdot 10^5 \frac{\text{kg}}{\text{ms}^2}$
Wall density	$\rho^w$	$1000 \frac{\text{kg}}{\text{m}^3}$
Fluid density	$\rho$	$1060 \frac{\text{kg}}{\text{m}^3}$
Length	l	0.4m
Soliton amplitude	a	0.00035m

These values are used in the equation (4.26) and solved using the spectral method. Three cases are considered:

1.  $\gamma = 0\text{s}, \kappa = 0\text{s}^{-1}$
2.  $\gamma = 0\text{s}, \kappa = 1\text{s}^{-1}$
3.  $\gamma = 10^{-4}\text{s}, \kappa = 0\text{s}^{-1}$

<sup>1</sup>There are different strategies for constructing different polynomials, such as the Chebyshev polynomial, but for now we will focus on the matrix derived from the Taylor series expansion. It goes without saying this is a huge and fascinating topic, and I only wish to give a small recollection of it here.

<sup>2</sup>For this study, ODE45 in Matlab was used

While these parameters are not physiologically derived, they are chosen to attempt to emulate a large blood vessel and serve for the purposes of investigating the models. Because of the unique soliton solutions in the KdV-BBM equation, which will propagate without change, it is natural to use these waves as a way to examine the effect of viscosity and viscoelasticity. Thus, all initial conditions are waves of the form

$$\eta(x, t) = 3 \frac{c_s - a}{b} \operatorname{sech}^2 \left( \sqrt{\frac{c_s - a}{4c_s c}} (x - c_s t) \right)$$

where

$$a = \tilde{c}, \quad b = \frac{5\tilde{c}}{2r_0}, \quad c = \frac{\tilde{c}(4\alpha + r_0)r_0}{16}$$

and  $c_s$  is the propagation speed of the wave. The wave is propagated until the final time  $t = 0.08\text{s}$ , with the results being show in Figure (5.1) As expected, for the inviscid fluid and

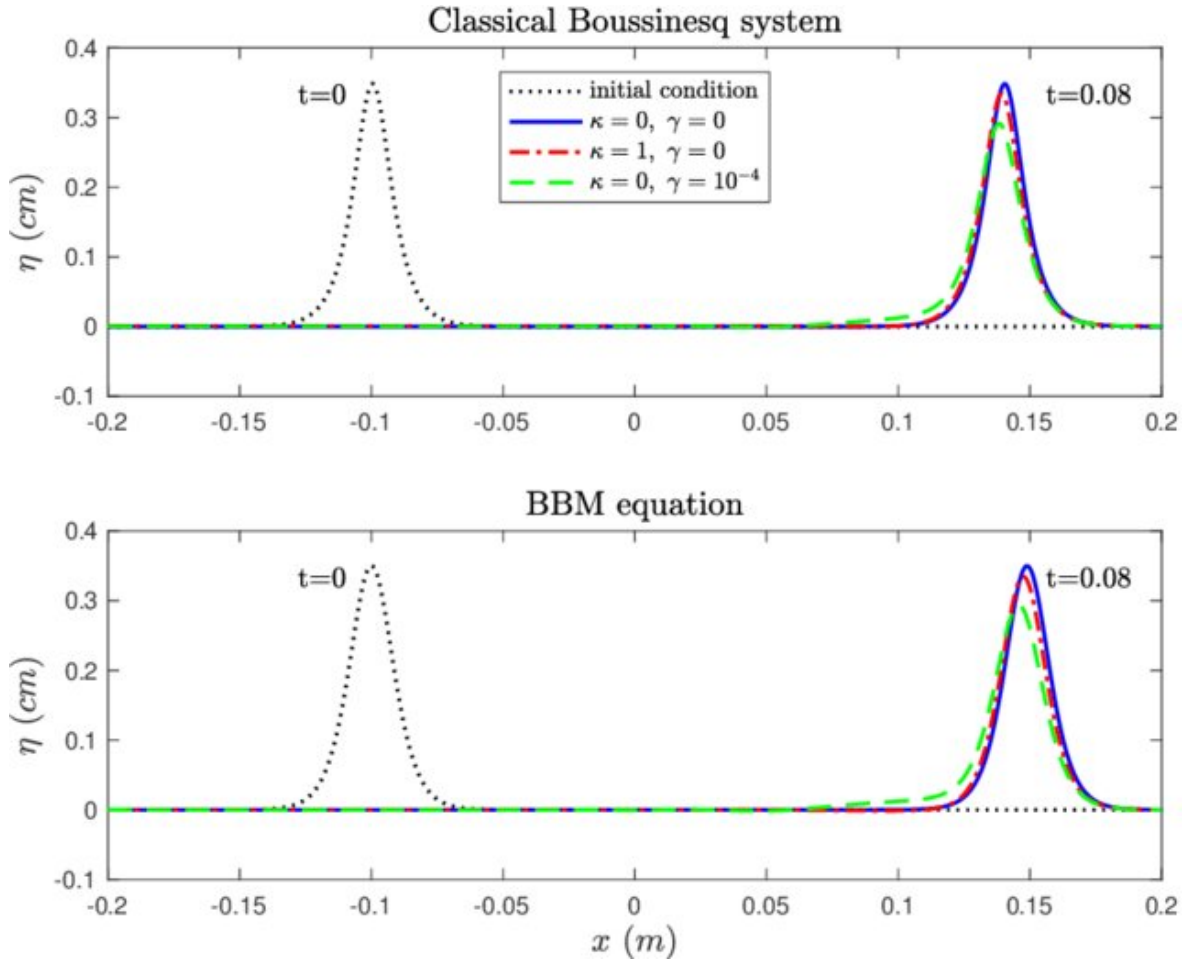


Figure 5.1: Results of the numerical experiments

purely elastic walls, the wave propagates without change in amplitude. When viscosity and viscoelasticity are introduced, the amplitude decreases by 6% and 17% respectively. In the case of the viscoelastic walls, the wave appears to broadens slightly. When both viscosity and viscoelasticity are accounted for at the same time, the amplitude decreases by 20%.<sup>3</sup> This

<sup>3</sup>The case for both nonzero  $\kappa$  and  $\gamma$  are not shown in Figure 5.1



indicates the large effects these two extra terms have on the overall propagation of waves in the arteries. In both cases, small amplitude waves propagate in the opposite direction, suggesting these models are capable of facilitating two-way propagation. This will prove useful for modelling of reflections.

## Chapter 6

# Conclusions

This thesis has investigated topics of methods in mathematical modelling. This was done by first showing derivations from first principles of behaviour of materials, then showing the necessary simplifications to obtain a tractible set of equations. A small history was discussed and some complications related to modelling introduced.

A new model was derived from asymptotic methods. By using this method, an equation was recovered whose use tends to be in water wave modelling - the KdV-BBM equation. Pulse wave propagation is an interesting newer application of these equations. A new term is introduced and justified in the analysis which accounts for viscoelasticity in the arterial wall. The effect of this term is investigated by considering the evolution of a soliton in the original KdV-BBM equation. How this soliton evolves when this viscoelasticity term is considered shows the effect of the new term. The effects of viscosity of blood and viscoelasticity of the arteries is clearly demonstrated and quantitatively show promise for new work.

Secondary to this, the equations can be solved quickly and with good stability by the Spectral Method, a dimension-reducing technique which involves using the Fourier Transform on the model equations, solving the transformed equation, and then performing an IFFT on the solution to recover the solution to the original equation. This method works with the KdV-BBM equation and the viscoelasticity term presents no complications with the Spectral Method, allowing it to simply slot into the equation and be solved in a straightforward manner.

# Bibliography

- [1] Frans N. van de Vosse and Nikos Stergiopoulos. Pulse wave propagation in the arterial tree. *Annual Review of Fluid Mechanics*, 43(1):467–499, 2011.
- [2] Yubing Shi, Patricia Lawford, and Rodney Hose. Review of zero-d and 1-d models of blood flow in the cardiovascular system. *BioMedical Engineering OnLine*, 10(1):33, Apr 2011.
- [3] Nikolaos Stergiopoulos. Computer simulation of arterial blood flow. 1990.
- [4] Otto Frank. The basic shape of the arterial pulse. first treatise: Mathematical analysis. *Journal of Molecular and Cellular Cardiology*, 22(3):255–277, 1990.
- [5] J. R. Womersley. Method for the calculation of velocity, rate of flow and viscous drag in arteries when the pressure gradient is known. *The Journal of Physiology*, 127(3):553–563, 1955.
- [6] J.J. Wang and K.H. Parker. Wave propagation in a model of the arterial circulation. *Journal of Biomechanics*, 37(4):457–470, 2004.
- [7] Alfio Quarteroni and Luca Formaggia. Mathematical modelling and numerical simulation of the cardiovascular system. In *Computational Models for the Human Body*, volume 12 of *Handbook of Numerical Analysis*, pages 3–127. Elsevier, 2004.
- [8] Sebastien Benzekry, Amanda Tracz, Michalis Matri, Ryan Corbelli, Dominique Barbolosi, and John M.L. Ebos. Modeling spontaneous metastasis following surgery: An in vivo-in silico approach. *Cancer Research*, 76(3):535–547, 2016.
- [9] Jeroen van Oostrum. *Applying Mathematical Models to Surgical Patient Planning*. PhD thesis, E, September 2009.
- [10] F.J.H. Gijzen, F.N. van de Vosse, and J.D. Janssen. The influence of the non-newtonian properties of blood on the flow in large arteries: steady flow in a carotid bifurcation model. *Journal of Biomechanics*, 32(6):601–608, 1999.
- [11] Dimitrios Mitsotakis, Denys Dutykh, and Qian Li. Asymptotic nonlinear and dispersive pulsatile flow in elastic vessels with cylindrical symmetry. *Computers & Mathematics with Applications*, 03 2018.
- [12] Y. Fung. *Biomechanics: mechanical properties of living tissues*. Biomechanics / Y. C. Fung. Springer-Verlag, 1981.
- [13] Luca Formaggia, Daniele Lamponi, and Alfio Quarteroni. One-dimensional models for blood flow in arteries. *Journal of Engineering Mathematics*, 47, 12 2003.

- [14] Anders Gabrielsen and Peter Norsk. Effect of spaceflight on the subcutaneous venoarteriolar reflex in the human lower leg. *Journal of Applied Physiology*, 103(3):959–962, 2007. PMID: 17585042.
- [15] C. Alberto Figueroa, Irene E. Vignon-Clementel, Kenneth E. Jansen, Thomas J.R. Hughes, and Charles A. Taylor. A coupled momentum method for modeling blood flow in three-dimensional deformable arteries. *Computer Methods in Applied Mechanics and Engineering*, 195(41):5685–5706, 2006. John H. Argyris Memorial Issue. Part II.
- [16] J.R. LaCourse, G. Mohanakrishnan, and K. Sivaprasad. Simulations of arterial pressure pulses using a transmission line model. *Journal of Biomechanics*, 19(9):771–780, 1986.
- [17] T. G. Myers, Vicent Ribas Ripoll, Anna Sáez de Tejada Cuenca, Sarah L. Mitchell, and Mark J. McGuinness. Modelling the cardiovascular system for assessing the blood pressure curve. *Mathematics-in-Industry Case Studies*, 8(1):2, Apr 2017.
- [18] Bessonov, N., Sequeira, A., Simakov, S., Vassilevskii, Yu., and Volpert, V. Methods of blood flow modelling. *Math. Model. Nat. Phenom.*, 11(1):1–25, 2016.
- [19] Vuk Milisic and Alfio Quarteroni. Analysis of lumped parameter models for blood flow simulations and their relation with 1d models. *Mathematical Modelling and Numerical Analysis*, 38, 07 2004.
- [20] Raheem Gul. Mathematical modeling and sensitivity analysis of lumped-parameter model of the human cardiovascular system, 05 2016.
- [21] Miguel Angel Fernández. Coupling schemes for incompressible fluid-structure interaction: implicit, semi-implicit and explicit. *Journal*, 55, 09 2011.
- [22] H. Schlichting. *Boundary-layer theory*. McGraw-Hill series in mechanical engineering. McGraw-Hill, 1979.
- [23] Martina Bukac and Suncica Canic. Longitudinal displacement in viscoelastic arteries: A novel fluid-structure interaction computational model, and experimental validation. *Mathematical biosciences and engineering : MBE*, 10:295–318, 04 2013.
- [24] A. QUAINI and A. QUARTERONI. A semi-implicit approach for fluid-structure interaction based on an algebraic fractional step method. *Mathematical Models and Methods in Applied Sciences*, 17(06):957–983, 2007.
- [25] Ruoya Wang and Rudolph L Gleason. A mechanical analysis of conduit arteries accounting for longitudinal residual strains. *Annals of Biomedical Engineering*, 38:1377–1387, 2010.
- [26] Effat Soleimani, Manijhe Mokhtari-Dizaji, Hajir Saberi, and Shervin Sharif-Kashani. A mathematical model for estimating the axial stress of the common carotid artery wall from ultrasound images. *Medical & Biological Engineering & Computing*, 54, 11 2015.
- [27] VA Dougalis and Dimitrios Mitsotakis. *Theory and Numerical Analysis of Boussinesq Systems*, pages 63–110. 02 2008.
- [28] L.N. Trefethen. *Spectral Methods in MATLAB*. Software, Environments, and Tools. Society for Industrial and Applied Mathematics (SIAM, 3600 Market Street, Floor 6, Philadelphia, PA 19104), 2000.

- [29] A. Bueno-Orovio, V. Pérez-García, and F. Fenton. Spectral methods for partial differential equations in irregular domains: The spectral smoothed boundary method. *SIAM Journal on Scientific Computing*, 28(3):886–900, 2006.